Chapter 5

Spectral Calculations with DFT

Ataf Ali Altaf, Samia Kausar and Amin Badshah

Additional information is available at the end of the chapter

http://dx.doi.org/10.5772/intechopen.71080

Abstract

Spectra calculations are an important branch of theoretical modeling, and due to the significant improvements of high-level computational methods, the calculated spectra can be used directly and sometimes help to correct the errors of experimental observations. On the other hand, theoretical computations assist the experimental assignments. The authors discuss three spectral calculations (UV-Vis, IR and NMR) that are the most widely used. UV-Visible spectrum can be carried out employing time-dependent density functional theory (TDDFT) with B3LYP/631G(d,p) and CAM-B3LYP functional method to illustrate the characteristics of vertical electronic excitations. The vibrational spectra can be generated from a list of frequencies and intensities using a Gaussian broadening function method. NMR chemical shifts can be calculated by density functional theory individual gauge for localized orbitals (DFTIGLO) method and by gauge including atomic orbitals (GIAO) approach.

Keywords: spectral calculation, vibrational spectra, DFT NMR calculation, TDDFT for UV-visible spectra

1. Introduction

Early days of quantum chemistry go back to Thomas-Fermi and Thomas-Fermi-Dirac models of the electronic structure of atoms, which gave the concept of articulating some parts or all of the molecular energy as a functional of the electron density, and then comes the traditional Hartree-Fock (HF) theory [1]. HF theory was a simplest ab initio technique and among the first principles of quantum-chemical theories, being attained directly from the Schrodinger-wave equation that did not incorporate any pragmatic contemplations. Although such theories and techniques proved beneficial, it was density functional theory (DFT) that laid a demanding theoretical foundation in 1964 by an outstanding result established by Hohenberg and Kohn [2].

The Hohenberg-Kohn theorems state that the exact ground state energy of the system is produced by a unique functional of the electron density ρ. The first theorem demonstrates a many-particle system n(x,y,z) for which one-to-one plotting happens between the ground state electric density and the ground state wave function. The second theorem verifies that total electric energy of the system E[n(x,y,z)] is minimalized by the ground state density [3]. The work of Kohn and Sham instantly surveyed and paved the way for hands-on computational applicability of DFT to physical systems, by linking a reference-state comprising of a set of noninteracting one-particle orbitals with a particular functional. The reference orbitals determined by a set of operative one-particle Schrodinger-wave equations are called Kohn-Sham (KS) equations [4]; one of them is depicted in Eq. (1).

$$\left(-\frac{1}{2}\nabla^2\left(\vec{r}\right)+V_{KS}\right)\Psi_i=\varepsilon_i\Psi_i \tag{1}$$

where V_{KS} is a local one-body potential defined as total density of the noninteracting system and is the same as the density of a real system.

2. Spectral implementations of DFT

The density functional theory (DFT) has become a powerful tool in computational chemistry owing to its usefulness. Spectroscopic analysis of chemical entities by this technique emerged as commanding implementation. Prediction of frequencies and spectral intensities by DFT calculations are indispensable nowadays for interpreting the experimental spectra of complex molecules. Much advancement has been made in the past decade to design new DFT approaches that can be employed into available quantum-chemical computational programs. For calculation of the molecular and electronic structures of ground-state systems and various spectral parameters related to NMR, ESR, UV-Vis and IR, various density functional practices are available now. Functionals available today can strive with best previous ab initio methods [5].

For experimental spectroscopists, theoretical computation of vibrational frequencies has become practically essential these days as specifically in problematic and uncertain cases it assists to assign and interpret experimental infrared/Raman spectra. Previously, the HF method was used in many studies to calculate vibrational frequencies, but it has long been identified that this approach miscalculates these frequencies even occasionally to a disturbing degree. Inadequate handling of electron correlation and anharmonicity of the vibrations are found to be the main contributions to error [6]. DFT largely overcome the errors as theoretical computations helped to interpret experimental conclusions depicting that using DFT these theoretical data can nearly be attained at the harmonic level. Calculation of optimized geometry, IR intensities, vibrational frequencies and Raman scattering activities can be done by employing different density functional approaches [7].

Taking NMR spectroscopy into consideration, DFT-based new methods are developed that are appropriate for the satisfactory hypothetical interpretation of NMR spectra of various chemical

and biochemical systems. It is obvious that local geometrical and electronic structures influence magnetic resonance parameters, i.e., shielding tensors, nuclear spin-spin coupling parameters, hyperfine tensors and g-tensors. For speculations of NMR parameters, a practical approximation of the real system is depicted by a model system in which 50–100 atoms are treated with ab initio techniques. Over the last years, DFT advanced by the capability to include effects of electron correlation in a very effectual means to the forefront of field of calculating NMR parameters [8, 9].

Competent calculations of excited states properties are emerging field of interest for quantum chemists; hence, they are developing interesting solutions for these properties. Because of advancement of computations based on the time-dependent density functional theory (TD-DFT) [10] in recent years, calculations of electronic structures in the excited states have become a motivation of interest. A commanding method of carrying out exact quantum mechanical calculations of the intervalence absorption spectrum is provided by the time-dependent concept of electronic spectroscopy. A corporeal picture of the effects of the coupling of electronic and nuclear motions became available by employing calculations in the time realm due to reason that the time development of the wave-packet can be tracked and inferred as well [11]. Plentiful successes of this technique have been recently revised as electronic spectra are often calculated with TD-DFT. Vertical excitation energies, absorption wavelength and oscillator strength calculations can be performed by this technique [12].

2.1. Theoretical vibrational spectra analysis

The influence of vibrational spectroscopy as an analytical tool in several fields is obvious. Qualitative association of bands and specific structures or chemical groups is basic interpretation of vibrational spectra. In contrast to nuclear magnetic resonance where nuclear spin is associated with one peak or multiplet is proved advantageous, united motion of all of the nuclei in sample is reason for observed bands in vibrational spectra. For N nuclei, there are at most 3 N-6 experiential fundamental bands and so far the matrix of internuclear force interactions, i.e., the second derivative matrix in harmonic approximation, has (3 N-6)(3 N -5)/2 exclusive terms. The extraction of force constants from vibrational frequencies is yet an undetermined mathematical problem as many bands are not actually observed; e.g., there are overtones, combination bands and nonconformities from the harmonic approximation; hence, the problem seems obstinate [13].

For the ground state's potential energy surface computation, discovery of effectual codes delivers a possible answer to the problem. A technique that will precisely determine the bonding, as well as intermolecular interactions, will be helpful for calculating vibrational spectra. The ground state properties and potential energies are accurately calculated by DFT approaches; therefore, DFT excellently and proficiently calculates the vibrational spectra from first principles [7]. The absolute values of the frequencies are high in contrast to experimental values while using DFT models as they seem to characterize the bonding pretty well and comparison with experimental trends is possible. DFT methods give sufficiently high accuracy of normal mode calculations as the restrictions of the harmonic approximation are often a foremost cause of divergence between theory and experiment.

It is reasonable to outspread the approach by including molecular interactions after given achievement of the method employed to small molecules. There are two aspects that can be reasons for inconsistency, i.e., anharmonicity and hydrogen bonding, both result in a lower frequency for a specific normal mode than projected by harmonic approximation [14].

2.1.1. *Spectral generation* via *Gaussian broadening function*

Computation of vibrational spectra of molecules in their ground and excited states can be done by using the Gaussian program. The program can also designate the dislocations of the molecule as it undergoes normal modes of vibrations along with prediction of spectral frequencies and intensities. The spectra can be produced from a list of frequencies and intensities employing a Gaussian broadening function as depicted in Eq. (2) [13]:

$$I(\nu) = \sum_{k}^{N} \frac{A_k}{\sqrt{2\pi\sigma}} exp\left\{-\frac{(v - v_0)^2}{2\sigma^2}\right\} \tag{2}$$

For each of the N vibrational modes calculated, intensity of each band is A_k in km/mol.

2.1.2. *Calculating the vibrational frequencies*

Study of a molecular system behind calculating the vibrational frequencies [7]. If springs are considered Hookean, for example, equations of motion can readily be solved when force is proportional to the displacement and we can find that vibrational frequencies are associated with force constants and masses of atoms. For instance, in a simple molecule like CO where there is only one spring, the frequency is calculated as in Eq. (3).

$$\nu = \frac{1}{2\pi}\sqrt{k/\mu} \tag{3}$$

where $\frac{1}{\mu} = \frac{1}{m_c} + \frac{1}{m_a}$ and k is the spring constant. The value of k can be computed from DFT calculations at equilibrium state, bond length $k = \frac{\partial^2 E}{\partial x^2}$. It is essential to perform geometry optimization prior to frequency calculations as these calculations are effective only at fixed points on the potential energy surface.

2.1.2.1. *Calculating second derivative of energy*

Before calculating the second derivative of energy, the first step in quantum chemical calculations is optimization of molecular geometry. Vibrational frequency calculations are done after optimizing geometry by using the same method and basis set as used for calculating vibrational frequency. Model's development is constructed on spontaneously rational values for interbond angles, bond distances and dihedral angles in the absence of experimental data. It is usually done by solving the following Schrodinger wave equation [15]:

$$\left(\widehat{H}_{el} + V_{NN}\right)\Psi_{el} = U\Psi_{el} \tag{4}$$

where $\widehat{H}_{el}$ is the one-electron Hamiltonian and V_{NN} is the operator of potential energy between the nuclei of molecular system intended for numerous molecular geometries to discover equilibrium geometry of the molecule, i.e., geometry optimization.

The second derivative of energy regarding the position of nuclei is factor on which molecular frequencies hinge on. Hartree-Fock theory, DFT-B3LYP and other approaches make available the analytic second derivative of energy. Input for frequency calculation is given by the optimized energy [16]. These derivatives are estimated at the equilibrium geometry with origin at the middle of mass by manipulating a set of second derivatives of molecular energy U respecting the 3 N nuclear Cartesian coordinates of a coordinate system as in Eq. (5) [15].

$$\left(\frac{\partial^2 U}{\partial X_i \partial X_j}\right)_{eq} \quad i, j = 1, 2, \ldots..3N \tag{5}$$

Mass-weighted force constant matrix elements give:

$$F_y = \frac{1}{\left(m_i m_j\right)^{1/2}}\left(\frac{\partial^2 U}{\partial X_i \partial X_j}\right)_{eq} \tag{6}$$

where m_i is mass of the nucleus in correspondence to coordinate X_i.

Then, set of 3 N linear equations in 3 N unknowns in Eq. (7) are being solved.

$$\sum_{j=1}^{3N}\left(F_{ij} - \delta_{ij}\lambda_k\right)I_{jk} = 0 \quad i, j = 1, 2, \ldots..3N \tag{7}$$

If coefficient of determinant vanishes, this set of consistent equations has a nontrivial explanation as follows:

$$\det\left(F_{ij} - \delta_{ij}\lambda_k\right) = 0 \tag{8}$$

This determinant is of order 3 N and on extension gives a polynomial whose highest power of λ_k is λ_k^{3N}, so the determinantal equation will yield 3 N roots (some of which may be the same) for λ_k.

2.1.2.2. Calculating vibrational frequencies

Calculation of molecular harmonic vibrational frequencies is now done as follows [15]:

$$v_k = \frac{\lambda_k^{1/2}}{2\pi} \tag{9}$$

By solving Eq. (9), six of the λ_k values originated will be zero giving six frequencies with zero value, in correspondence to the three translational and three rotational degrees of freedom of

molecule. In practice, one may find six vibrational frequencies with values almost zero because equilibrium geometry never originates with infinite precision. The remaining 36-*N* vibrational frequencies depict molecular-harmonic vibrational frequencies.

2.1.2.3. Zero-point energy calculations for maximum vibrations

Zero-point energy is defined as the sum over all the vibrational modes for a molecule with maximum number of vibrational modes and calculated as:

$$E_{ZPE} = \sum_i \frac{1}{2} h\nu_i \tag{10}$$

2.1.3. Normal coordinate analysis

Normal coordinate analysis gives comprehensive explanation of vibrational modes. It is termed a practice that calculates the vibrational frequencies involving observed frequencies of more preferably infrared and Raman harmonic frequencies to equilibrium geometry, force constants and atomic masses of an oscillating system. In assigning vibrational spectra, normal coordinate analysis proved beneficial, but reliable intramolecular force constants influence its predictive ability [17].

2.1.4. B3LYP density functional method

DFT syndicates accuracy with computational rapidity and user-friendliness for investigating the ground state characteristics in sturdily bound systems. Consistent highly reliable hybrid DFT methods (discussed in Section 3.1) make them more proficient and endearing. B3LYP functional [18] (discussed in hybrid methods of Section 3.1) is the most extensively used among all hybrid density functional methods as it is considered to give most exact vibrational frequencies of compounds only if calculated frequencies are scaled by a uniform scaling factor. Scaling is done to compensate for all probable causes of inaccuracy produced owing to electronic structure method–related inaccuracies, e.g., basis set insufficiencies and estimated handling of electron-correlation and nuclear motion treatment inaccuracies [19].

2.1.5. IR calculations in Gaussian software

Gaussian is a most employed computational chemistry software program, whereas Gauss View is an inexpensive full featured graphical user interface for Gaussian. One can submit inputs to Gaussian and can observe output graphically, which is usually produced by Gaussian software via using Gauss View. For IR spectrum calculations in Gaussian, the following are the steps:

i. After predicting the number of vibrational modes and expected regions for frequencies for molecule by theoretical calculations, build molecule in Gauss View. Go to Calculate from Gauss View toolbar and select Gaussian. In the Job Type dialog box, select Opt + Freq and optimize to a 'Minimum' Calculate Force Constants-'Never,' Compute Raman- 'Default,' deselect any other option.

ii. In Method section, select ground state (HF, Restricted or DFT Restricted and B3LYP according to required calculation) and select a basis set, Charge-0 and Spin-Singlet. Insert SCF = Tight in the Additional Keywords section and if your calculation is in vacuo, select 'None' in the Solvation dialog box. Submit the calculation.

iii. Open the output file of the optimized structure in Gauss View. Verify that the optimization calculation has converged by checking that the maximum force, RMS force, maximum displacement and RMS displacement parameters are all converged.

iv. Go to Results and select the 'Vibrations' option. View the IR spectrum by pressing the 'Spectrum' button and check out whether the number of modes are in accordance with theoretical calculations or not. Each vibrational mode can be visualized by highlighting it in the 'Display Vibrations' table and pressing the 'Start' button.

3. DFT methods for nuclear magnetic resonance (NMR)

NMR is based on the principle that the energy of a system containing nuclear or electron magnetic moments arising from the spin of a particle, in the existence of an external stationary magnetic field, depends upon the direction of the magnetic moment with respect to the external field. One can thus measure the energy difference for different directions of the electronic magnetic moment (electronic Zeeman effect) or of nuclear magnetic moment (nuclear Zeeman effect) by employing a suitable oscillating external magnetic field as a probe [20].

NMR parameters are considered as quantities which are determined shifts, indirect spin-spin coupling constant and direct dipole-dipole coupling constants. This electronic structure in turn confidentially interrelated to local and global geometry and hence internal flexibility and intramolecular interactions influences NMR parameters. Chemical shifts along with spin-spin coupling constants found an average experimentally in comparison to those values belonging to all geometrical arrangements arising throughout the sequence of NMR experiment. Unfortunately, chemical shifts are generally found to be dependent on the internal dynamics or on the intermolecular interactions in various descriptions. Consequently, for obtaining structural information, most experimental NMR techniques imply coupling constants or the nuclear Overhauser effect instead of chemical shifts. However, ab initio calculations provide the understanding to structure-chemical shifts or spin-spin coupling constant associations, which can make the experimental data interpretation much easier in this sense. That is the reason that highly capable and steadfast computational calculations are in high demand [21].

As commonly noted that, when results of sufficient quality are attainable by employing various strategies based on wave function properties. These procedures are restricted to small- and medium-sized systems unfortunately. With the advancements of density functional methods, it is possible to acquire pertinent results even for larger molecules, such as fragments of proteins and nucleic acids [22] where the electron correlation effects are

indirectly accounted through the exchange-correlation functional. DFT-based NMR calculations have seen a rapid expansion during the last 10 years—that is perhaps best designated with the word explosion. Since the publication of these calculations, methods have already entered the standard repertoire of quantum chemistry in short time length. More comprehensive and technical as well as more general reviews are available as theoretical portrayal of NMR chemical shifts based on the more traditional ab initio procedures has seen a marvelous progress as well [23]. For NMR calculations, density functional theory (DFT) is recently proved to substitute the traditional Hartree-Fock (HF) and post-HF methods [24]. Inclusion of electron correlation effects in a very efficient way to calculate NMR parameters is a rather new field of application in DFT over the last years.

3.1. Calculations of NMR parameters

Total energy E of an n-electron system is expressed exactly on the basis of DFT approach as in Eq. (11) [2].

$$E = \sum_{i}^{n} \int d\vec{r} \Psi_i^* \left(\frac{p^2}{2} + V_N \right) \Psi_i \frac{1}{2} \int d\vec{r^1} \vec{r^2} \frac{\rho\left(\vec{r^1}\right)\rho\left(\vec{r^2}\right)}{|\vec{r^1} - \vec{r^2}|} + E_{XC} \tag{11}$$

In Eq. (11), the $\{\Psi_i\}$ is a set of n orthonormal one-electron functions, $\rho = \sum_{i}^{n} \Psi_i^* \Psi_i$is electronic density of the system, V_N is the external (nuclear) potential, and $\vec{p}$ is momentum operator. Hence, the kinetic and potential energy of a model system with the same density is signified by the first integral but without incorporating electron-electron communication. The second term represents itself as coulomb interaction of electron density. The XC energy and E proper (E_{XC}) are functionals of the density although exact functional arrangement for E_{XC} is not known (defined through Eq. (11)). Any application of DFT is mainly concerned with the assessment of numerous approximations; hence, Kohn-Sham (KS) equations are typically derived from Eq. (11) [4, 25].

$$h_{KS}\Psi_i = \varepsilon_i \Psi_i \tag{12}$$

$$h_{KS} = \frac{p^2}{2} + V_{KS} = \frac{p^2}{2} + V_N + \int d\vec{r} \frac{\rho\left(\vec{r^2}\right)}{|\vec{r^1} - \vec{r^2}|} + V_{XC} \tag{13}$$

The XC potential V_{XC} is the functional derivative of the XC energy E_{XC} with respect to the density, ρ. The inclusion of magnetic fields is another extension, which can be introduced. Obviously, this is essential to all the properties to be introduced. The magnetic field $\vec{B}$ is most accessibly acquaint with supposed minimal coupling as in Eq. (13) [26].

$$\vec{p} = \vec{p} + \vec{A}/c \tag{14}$$

where $\vec{A}$ is the vector potential of the field. Though this is not the entire division in DFT. Rather, the XC energy (E_{XC}) becomes a relativistic for current density functional, which interprets in nonrelativistic system to the electron density ρ and the current density $\vec{j}$ depicted in Eq. (14) [27].

$$E_{XC}[p] \xrightarrow{substitute} E_{XC}\left[p, \vec{j}\right] \tag{15}$$

3.1.1. Exchange-correlation functional

Quality of the description centers exclusively on precision of the approximation to Exc as mentioned earlier that obvious form of the exchange-correlation functional (Exc) is not identified yet. Unfortunately, there is no systematic mode of improving exchange-correlation functionals although the pursuit for improved and better functionals is at the very core of DFT. Prevailing XC functionals can be roughly categorized into three distinct groups [28] as several approximations used for Exc are as follows:

3.1.1.1. The local density approximation (LDA)

The idea of a nonvariating electron gas laid the foundation of this model, which approximates Exc in turn written as:

$$E_{XC}^{LDA}[\rho] = \int \rho(r)\epsilon_{xc}[\rho]dr \tag{16}$$

$\epsilon_{xc}[\rho]$ is the exchange-correlation energy per particle of a uniform electron gas of density ρ(r) in Eq. (15). The $E_{XC}^{LDA}[\rho]$ can be correctly split into exchange and correlation parts as:

$$E_{XC}^{LDA}[\rho] = E_X^{LDA} + E_C^{LDA} \tag{17}$$

3.1.1.2. The generalized gradient approximations (GGA)

The generalized gradient approximations (GGA) for Exc are not lone functions of local density ρ(r) but also functions of the gradient of charge density ∇ρ(r) in comparison to LDA. They can be generically inscribed as:

$$E_{XC}^{GGA}\left[\rho_\alpha, \rho_\beta\right] = \int f\left(\rho_\alpha, \rho_\beta, \Delta\rho_\alpha, \Delta\rho_\beta\right)dr \tag{18}$$

α and β denote to "up" and "down" spin, respectively, in Eq. (17). Now, E_{XC}^{GGA} is also typically split into its exchange and correlation parts as:

$$E_{XC}^{GGA}[\rho] = E_X^{GGA} + E_C^{GGA} \tag{19}$$

The GGA exchange functional's representatives are functionals by Becke, 1988 (B or B88) [18] and by Perdew and Wang, 1986 (P or PW86) [29] and are the most familiar ones. Perdew and Wang also established the PW91 exchange-correlation functional [30] comprising exchange

and correlation contributions; if used separately, both functionals are symbolized by PW91. The exchange fragment of PW91 is analogous to B88 and the correlation part is a modified form of P86. Currently, possibly the most prevalent correlation functional accounts to contributions of Lee et al. (LYP) [31]. Because of presence of some indigenous components, it differs from the other GGA functionals.

3.1.1.3. The hybrid methods

Exchange-correlation functionals in which exchange part is composed of particular Hartree-Fock exchange and pure density functionals for exchange are called hybrid functionals. These functionals consist of a mixture of Hartree-Fock exchange with DFT exchange and correlation in other words as depicted in Eq. (19).

$$E_{XC}^{hybrid} = c^{HF}E_X^{HF} + c^{DFT}E_C^{DFT} \tag{20}$$

3.1.1.4. Becke's three-parameter hybrid functional (B_3LYP) method

An illustrative example of the above-mentioned hybrid representations is Becke's three-parameter hybrid functional (B3), depicted in Eq. (20). [18], and exchange energy is being calculated by using this (B3) functional. If correlation functional LYP or PW91 is assumed for E_C^{GGA}, B3LYP or B3PW91 will be obtained, respectively. The earlier mentioned is most widely used exchange-correlation functional nowadays, and in many research domains throughout, it was also rigorously active. Since GGAs are better in comparison to LSDA, they could also employ a functional form like this (B3) as follows:

$$E_{XC}^{B3} = (1-a)E_X^{LSDA} + aE_X^{HF} + b\Delta E_X^{B88} + (1-c)E_C^{LSDA} + cE_c^{GGA} \tag{21}$$

B_3LYP uses this formulation, with LYP for ΔE_c^{GGA}.

3.2. Shielding tensor calculations

The most basic DFT calculations of NMR chemical shifts were done years ago in which very small basis sets were employed and inappropriate approximation to the exchange-correlation (XC) functional was done due to which point of practical applicability was lost. Also in any handling of magnetic fields, another central exertion that surfaces is the so-called gauge problem [28] be it in DFT or otherwise.

3.2.1. Solving gauge problem

The gauge requirement should disappear just as any anticipation value together with NMR possessions that can only hinge on the values of observable quantities. Certainly, this is the case for particular solutions of, for example, the KS equations, Eq. (12a, b) where large (immeasurable) basis sets are employed. A strong dependence on the choice of gauge is of main concern for approximate solutions with smaller (infinite) basis sets. Current applications of DFT for calculating NMR chemical shifts have used density functional theory individual gauge

for localized orbitals (DFTIGLO) method [9] and gauge including atomic orbitals (GIAO) approach [32].

3.2.2. The GIAO method

One appraises matrix fundamentals of the Hamiltonian in terms of a basis of field-dependent atomic orbitals (AO) in the GIAO method. By insertion of an intricate phase factor denoting the position of basis function, which is usually nucleus, the basic functions are made obviously dependent on the magnetic field. Such orbitals are termed as London atomic orbitals (LAO) or the gauge including atomic orbitals (GIAO). Matrix elements involved in GIAOs only differentiate in the vector potentials is the essence of idea, in that way entirely eradicating the reference to a complete gauge origin. Employment of field-dependent GIAOs as basic functions [33] is possibly the best solution to the gauge problem.

$$\chi_a\left(\vec{B}, \vec{r}\right) = exp\left[\frac{i}{2c}\left(\vec{B}x\vec{R}_a\right).\vec{r}\right]\chi_a\left(\vec{r}\right) \tag{22}$$

where $\underset{a}{\vec{R}}$ and $\chi_a\left(\vec{B}, \vec{r}\right)$ are the conforming GIAO and $\chi_a\left(\vec{r}\right)$ is customary field-free basis function that is adjusted at position. The field-dependent prefactor Eq. (21) guarantees that only differences of position vectors give the impression in expectation values. This eradicates any origin dependence, even for estimated MOs and finite basis sets. For showing the complete basis set limit, correspondence of the GIAO and the simpler common gauge methods to the NMR shielding are depicted. Nucleus-attached basis functions in geometry optimization processes have been equated with specific AOs (Eq. (21)) by assigning a field-dependent phase factor to them.

Working equations for the NMR shielding tensor ($\vec{\sigma}$) can be derived from the GIAO formulation of Eq. (21). The absolute shielding σ is interrelated to the more acquainted chemical shift δ as follows [33]:

$$\delta = \sigma_{ref} - \sigma \tag{23}$$

where σ_{ref} is the absolute shielding of reference compound (e.g., tetramethylsilane [TMS] for ^{1}H, ^{13}C and ^{29}Si NMR). Opposite sign between δ and σ can be noted, whereas GIAO shielding tensor is specified in DFT as [34]:

$$\vec{\vec{\sigma}} = \vec{\vec{\sigma^p}} + \vec{\vec{\sigma^p}} \tag{24}$$

where $\vec{\vec{\sigma}}$ has been divided into its paramagnetic and diamagnetic fragments. Generally, this division is not exceptional as only the total shielding is an apparent quantity, but for the GIAO method, it has been defined exclusively.

3.2.3. The IGLO method

The use of disseminated gauge origins was depicted by the individual gauge for localized orbitals method (IGLO) [9], which was the first to empower the organized learning of nuclear shielding in larger systems. Evaluation of shielding tensor in terms of localized molecular orbitals (MO) is the idea of approach. To minimalize the absolute value of paramagnetic involvement, individual gauge origins of shielding tensor are selected. In the IGLO method, local phase factors are involved to molecular orbital in comparison to the GIAO approach where a phase factor is associated to each atomic orbital. In computational analysis point of view, IGLO approach is less challenging in contrast to the GIAO method since the use of distinct approximations of derivative two-electron integrals by this approach is most probable. By using localized orbitals, previously mentioned approximations are empowered; hence, it is important to select an appropriate basis set in an IGLO calculation [35]. According to IGLO approach, it is possible to allot comparable exponential prefactors to other objects, e.g., to localized MOs as a replacement for GIAO method. In IGLO method, specific integrals are easier to estimate analytically. Gauge difficulty has been resolute recently by retaining numerical integration or by techniques that were used in geometry optimization measures.

3.3. Nuclear spin-spin coupling constant calculations

Highly appropriate ab initio calculations of spin-spin coupling constants are still very infrequent and usually deal with the simplest molecules only in comparison to excessive advancement in concept and computer codes for shielding tensor scheming. Shielding tensors are the reasons behind sensitivity of nuclear spin spin coupling constants to the correlation effects and basis set quality [36]. There are four significant contributions which causes other problems to the nuclear spin-spin coupling constants, are enlisted as follows:

a. Fermi contact (FC),

b. Paramagnetic spin orbit (PSO)

c. Spin dipolar (SD)

d. Diamagnetic spin orbit (DSO)

HF calculations of the spin-spin coupling constants of large molecules lead to deprived contract with experimental numbers and further empirical scaling has to be done. On the other hand, the use of post–Hartree-Fock methods and prolonged basis sets for demanding handlings of all the four contributions is very inefficient and time-consuming.

In DFT, only a single paper by Fukui [23] published years ago was worthy initially, where the blend of finite perturbation theory (FPT) and the LCAO-Xa method was employed and only calculations of the FC contribution to the spin-spin coupling constant were carried out, which gave somewhat poor results likely as too poor basis set in combination with the Xa potential was used. As in Ref. [37], a new method to calculate the nuclear spin-spin coupling tensor using DFT procedure is developed sideways to the shielding tensor calculations in accordance.

The portrayal of calculations follows Ref. [37]. By meaning, the nuclear spin-spin coupling tensor $J_{MN_{uv}}$ is the second derivative of the total energy of the system with respect to the spins of the nuclei M and N as depicted in Eq. (24).

$$J_{MN_{uv}} = \left[\frac{\partial^2 E(I_{Mu}.I_{Nv})}{(\delta I_{Mu}.\delta I_{Nv})}\right]_{I_{Mu}=I_{Nv}=0} \qquad u, v = \{x, y, z\} \tag{25}$$

The orientationally averaged value of the nuclear spin-spin coupling tensor ($J_{MN_{uv}}$) of nuclear spin-spin coupling constant (J_{MN}) is the focus of interest in many cases.

$$J_{MN} = \frac{1}{3}\left(J_{MN_{xx}} + J_{MN_{yy}} + J_{MN_{zz}}\right) \tag{26}$$

3.4. Chemical shift calculation from DFT-B_3LYP-GIAO method

Since calculations for TMS are encompassed in many software, DFT-B_3LYP-GIAO is the 6-311 + G(2d.p) [38], a suitable basis set, which easily determines the chemical shifts relative to TMS. The use of smaller 6-31 + G(d,p) basis set for calculations is most suitable for students compared to larger basis sets such as the 6-311 + G(2d,p) or even the very large 6-311++G (3df,3pd) basis sets that are employed for research purposes on small molecules. Many of the movements necessitate much less than 3 hours fixed for a standard research laboratory session even while using the larger basic sets. First of all, in this method, the structure is optimized in all the cases, and then to establish that either optimized structure is at least a local minimal or not, vibrational frequencies are determined. After the complete optimization of the structure, shielding constants are calculated using the GIAO method. Calculations for chemical shifts are carried out by subtracting the value of the screening constant (σ), which is calculated from the value of the screening constant calculated for TMS using the same level of theory [38].

$$\delta = \sigma_{TMS\_}\sigma_{Calculated} \tag{27}$$

3.5. NMR calculation steps using Gaussian software

Basic considerations in NMR calculations are as follows: first, how many types of protons are there in molecule and which are they and second, how many NMR signals are expected to see and in which regions. In the case of an NMR spectrum calculation, geometry optimization calculation is needed first of all and then optimized structure is used to perform NMR spectrum calculation using the same method and basis set.

i. Follow the calculations in Section 2.1.5 till step i for geometry optimization calculations and then follow steps used to perform an HNMR spectrum calculation of the optimized structure with the same method and basis set.

ii. Press the Calculate button in the Gauss View toolbar and select Gaussian. In the Job Type dialog box, select 'NMR' and 'GIAO method. Submit the calculation after checking all parameters. Open the output file and select the NMR option from Results.

iii. In the 'SCF GIAO magnetic shielding dialog box, select 'H' option in Element drop-down list, and in the Reference list, select the calculation method earlier used. The number of peaks of magnetic shielding observed is noted. Infer calculated spectrum and compare it with theoretical calculations. With this, multiplicity of the peaks, temperature at which NMR experiment is simulated and width of the NMR peaks can be discussed.

iv. Open the log file and search for or scroll to the line "SCF GIAO Magnetic Shielding tensor (ppm)." For simple NMR experiments, the signals are found at the chemical shifts, which appear after the heading "isotropic." All other numbers relate to the directionality of the NMR signals.

4. Time-dependent density functional theory (TD-DFT) for UV-vis spectra

As classic DFT is concerned with ground stationary state and applications, i.e., UV-vis spectroscopy, photochemistry, NLO and others, comprise either electronic excited states or time-dependent electronic characteristics, which are in agreement with time-dependent density functional theory (TD-DFT). From classic paper of Runge and Gross [39], formal TD-DFT is traced back, which strained to firm up former efforts on the same topic. Therefore, Runge-Gross TD-DFT is two decades younger than Hohenberg Kohn-Sham theory [2], which is about stationary ground state as mentioned earlier. Four theorems proposed in the Runge-Gross paper. First, Runge-Gross theorem states that external potential up to an additive function of time is regulated by time-dependent charge density, $\rho(r,t)$, in cooperation with preliminary wave function (Ψ_0).

Various chemical and physical molecular properties provide basis for electronic spectra. Different chemical and physical effects can easily be computationally investigated by modifying the spectral characteristics of molecules as many stimulating chemical problems are included in both ground and excited states of molecules. As for ground state properties of atoms, molecules and solids, DFT gave an effective explanation; hence, in order to designate photochemical and photophysical procedures, DFT formalism has to be expanded to excited states. So, for excited state calculations, time-dependent DFT (TD-DFT) is established as an operative tool [40] as it provides first principle technique for calculating excitation energies and various response-related characteristics in density functional outline.

There are classically one or more low energy excited states for a molecule that can be designated as valence-MO-valence-MO single electronic excitations and replicated in spectra. Energies of excited determinants are essential for multiplet energy calculation such as employing spin-orbital number (i) to the empty spin-orbital number (j). Accordingly, specific states are denoted as $\pi \rightarrow \pi^*$, $n \rightarrow \pi^*$ transitions. Relative easiness of character sometimes smoothes the process of concluding wave functions for these states. The calculation of the dynamic answer of charge density proposes a rigorous direction to time-dependent simplification of DFT formalism. The poles of dynamic polarizability regulate excitation energies permitting the

determination of electronic excitation spectrum in typical dipole approximation [41]. The poles' strengths are provided by oscillator strengths (f_i) or by transition dipole moment (μ_i) consistently also termed as intensity of the optical transitions.

4.1. Absorption spectra calculation

Electronic absorption spectra calculation is foremost applicability of TD-DFT after the geometry got optimized by using linear response theory. First, the Hohenberg-Kohn theorem statement that dynamic linear response of a system of N-electrons is determined by the ground-state charge density was discussed earlier but no applied mean was found to build this response. A productive procedure was provided by TD-DFT from which absorption spectra can be calculated by following steps [42]:

Step 1: The calculations comprised of promulgating Kohn-Sham orbital incidence of a trivial dynamic perturbation, e.g., considering system being perturbed by Eq. (27).

Step 2: Then induced dipole moment, $\mu_{induced}(t)$, is calculated by Eq. (28), which depicts the difference among time-dependent and permanent dipole moments of a system.

Step 3: Dynamic polarizability, α, is expressed by linear term, $\mu_{induced}(t) = \int \alpha(t - t')\varepsilon(t)$.Final calculations of dynamic polarizability in Eq. (29) are carried out after applying Fourier transform convolution theorem.

Step 4: Sum-over-states (SOS) form of dynamic polarizability has the form:

$$v_{applied}(r,t) = \varepsilon(t).\boldsymbol{r} \tag{28}$$

$$\mu_{induced}(t) = -e\int \boldsymbol{r}n(r.t)\boldsymbol{r}d \tag{29}$$

$$\alpha(\omega) = \mu(\omega)/E(\omega) \tag{30}$$

$$\alpha(\omega) = \sum_{I\neq 0}\frac{f_I}{\omega_I^2 - \omega^2} \tag{31}$$

where ω_I and f_I are corresponding vertical excitation energies and conforming oscillator strength.

Finally, spectrum was obtained employing Eq. (31) also termed as Lorentzian broadened stick spectrum:

$$S(\omega) = \frac{2\omega}{\pi}Im\alpha(\omega + i\eta) \tag{32}$$

Such a procedure has been executed in many computer codes, e.g., in Octopus code [43], and has benefited that absorption spectrum of a very huge molecule over a wide range of energies can be calculated even though using only reasonable spectral resolution. This function parallels to optical absorption spectrum, e.g., calculating spectra of benzene [44] by TD-DFT approach depicted in **Figure 1**.

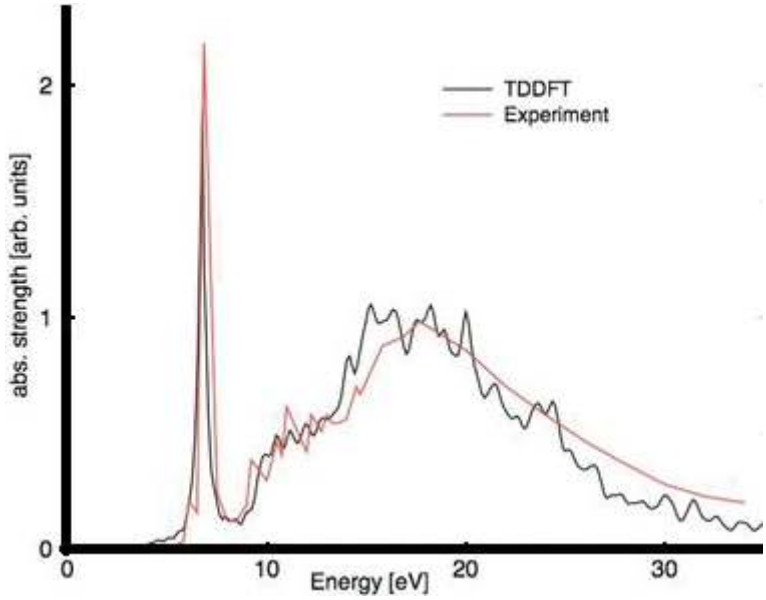

Figure 1. Absorption spectra of benzene.

4.1.1. Calculating the oscillator strength

It is an important point to note that TD-DFT calculations not only give excitation energies (ω) but also provide respective oscillator strengths. Oscillator strengths are actually pure numbers in a complete basis set [42].

$$f_I = \frac{2m_e}{3h}\omega_I|\langle 0|r|I\rangle|2 \tag{33}$$

Obviously, $\omega = E_I - E_0$ is an excitation energy in the case of $|I\rangle\langle 0|$ and $\omega = E_0 - E_I$ is a de-excitation in the case of $|0\rangle\langle I|$. To more simply relate the molar extinction coefficient (ε) in an absorption experimentation, Eq. (32) has been consciously expressed in Gaussian instead of atomic units. In SI units, frequency spectrum is assumed to first approximation [42] by:

$$\epsilon(v) = \sum_I \frac{N_A e^2}{4m_e c\ \ln(10)\epsilon_0} S(v - v_I) = \left(6.94 \times 10^{+18}\frac{L}{cm}.s\right)\sum_I S(v - v_I) \tag{34}$$

where S(ν) is a spectral shape function usually a Gaussian whose full width at half maximal is determined through experiment with area normalized to unity, whereas N_A depicts the Avogadro's number.

Absorption spectrum frequently results by excitations having larger oscillator strength because absorption peaks are often scaled with oscillator strength (f_I) of the excitation. Excitations with small oscillator strength (f_I) are also omitted from final spectrum while fundamentally working

on oscillator strength carrying subspace so that absorption spectrum is possibly calculated with less excitations in a fixed energy space. A common problem considered is that a large number of excitations have to be estimated with the purpose of covering energy space of concentration, while figure of absorption spectrum is determined by only some of them because of their greater oscillator strength (f_I) [45].

4.1.2. Calculating the intensity of absorption

Another detailed DFT method is presented, proposed in ref. [46], to calculate UV absorption spectra. The integration is completed over real $\vec{r}$ space. Intensity of absorption is in direct proportion to transition dipole moment $\vec{\mu_{jk}}$ from ground *j*th to *k*th excited state; hence, it can be estimated by formula [47]:

$$I_{jk} \approx \omega_{jk} \frac{\left(\mu_{jk}\right)2}{\hbar\omega_{jk} - \hbar\omega \pm i\Gamma_{jk}} \tag{35}$$

where $\hbar\omega$ is the input running radiation energy and $\hbar\omega_{jk}$ is energy difference between ground (j) and excited (k) state. Γ_{jk} is termed as line broadening, which is characterized by electron vibration broadening and inversely proportional to the period of k state.

4.1.3. Emission spectra calculation

As high harmonic generation is possible with TD-DFT methods, emission spectra [48] are calculated by:

$$\sigma_{emision}(\omega) = \left| \int dt e^{i\omega t} \frac{d^2}{dt^2} d(t) \right|^2 \tag{36}$$

4.2. Linear response TD-DFT(LR-TD-DFT) and absorption spectrum

Absorption spectrum is the fundamental property of a system. One working on absorption spectra calculations is mainly concerned with the lowest excited states commonly. Though, excitations over a broader energy range may be essential, consequentially requiring very challenging calculations while working for large molecular complexes and high density of states (DOS) materials [49]. Hence, for large systems approximate, precise and efficient computational methods have to be looked for. LR-TD-DFT is extensively employed to compute absorption spectra of larger systems as well [50]. To estimate the absorption spectrum in full LR-TD-DFT context, a two-sided Lanczos process is proposed in Ref. [51]. To acquire an accurate estimation of absorption spectrum, a more standard Lanczos algorithm with an appropriately selected inner product was employed.

4.2.1. LR-TD-DFT formulation

Density response of a system by applying an external time-dependent perturbation in linear response formulation of TD-DFT (LR-TD-DFT) is usually studied as [52]:

$$\rho(\boldsymbol{r},t) = \rho_0(\boldsymbol{r}) + \boldsymbol{\delta}(\boldsymbol{r},t) \tag{37}$$

In chemistry, LR-TD-DFT equations are articulated in matrix arrangement using the Kohn-Sham basic formulation. First-order density response δρ(**r**, t) can be extended on the basis of unperturbed orbitals. Linear response of the electronic density articulated in matrix form is depicted as:

$$\delta\boldsymbol{\rho}_{ij}(t) = \int_{t0}^{t} dt' \sum_{kl} \delta v_{kl}(t')\chi_{ij,\ \ kl}(\boldsymbol{r},t,\boldsymbol{r}',\boldsymbol{t}') \tag{38}$$

In Fourier space, it is represented as:

$$\delta\boldsymbol{\rho}_{ij}(\omega) = \sum_{kl} \delta v_{kl}(\omega)\chi_{ij,\ \ kl}(\omega) \tag{39}$$

The connection between Kohn-Sham response function and particular density response function is efficiently stated in terms of the inverse of their conforming Fourier transform time, $t_2 - t_1$ as follows:

$$\chi^{-1}(\boldsymbol{r},\boldsymbol{r}',\omega) = \chi_s^{-1}(\boldsymbol{r},\boldsymbol{r}',\omega) - \frac{1}{|\boldsymbol{r}_1 - \boldsymbol{r}_2|} - f_{xc}(\boldsymbol{r}_1,\boldsymbol{r}_2\omega) \tag{40}$$

In summary, locating excitation energies of the interacting system is problematic, and poles of the response function give the way to calculate excitation energies.

$$\{f_I,\omega_I\} \Rightarrow poles\ of\ \chi(\omega)$$

Actually, χ(ω) has poles at correct excitation energies ω_I. From this point, calculations for absorption spectra follow the route as explained in Section 4.1. Computation of the dynamic dipole polarizability [α(ω)] is a noninteracting response of specific interest in calculating absorption spectra, which is a response function that relays external potential to the change in dipole as depicted in Section 4.1. The Fourier transform of the dynamic dipole polarizability can be written as in Eq. (29). Excitation energies (ω_I) are calculated by poles of the dynamic polarizability [53], while the oscillator strengths are determined by residual (f_I) [52].

Calculating the absorption spectrum with LR-TD-DFT method also includes resolving a non-Hermitian eigenvalue problem; therefore, the absorption spectrum is attained as [50]:

$$\sigma(\omega) = \frac{1}{3}\sum_i f_i^2 |\delta(\omega - \lambda_i) - \delta(\omega + \lambda_i)| \tag{41}$$

4.3. Electronic calculations using Gaussian software

TD-DFT method in Gaussian makes it practical to study excited state systems since it produces results that are comparable in accuracy to ground-state DFT calculations. Natural transition orbitals (NTOs) can be a helpful way of obtaining a qualitative description of electronic

excitations. They do so by transforming the ordinary orbital representation into a more compact particle (occupied) to empty hole (unoccupied) [54].

i. First step follows the calculations presented in Section 2.1.5 till step i for geometry optimization calculations and then follow steps used to perform TD-DFT calculation of the optimized structure for UV-Visible spectral calculations. Solvent can be added using TD (singlets, nstates).

ii. Calculate the absorption spectrum. Compare the calculated absorption spectra (lambda max) with the experiment taking f > 0.0. Basis set/methods can be changed to generate spectrum in good agreement with theoretical assumption.

Generating NTOs:

i. Run an excited state calculation, saving the checkpoint file.

ii. Examine the calculation results to determine the excited state of interest.

iii. Run a single point calculation to generate the NTOs for the desired excited state. This step can be repeated to view focusing excited state.

5. Examples illustrating vibrational calculations

In our work [55], we have synthesized 1,3-diisobutyl thiourea ($C_9H_{20}N_2S$) and its vibrational analysis was carried out using DFT methods. Theoretical calculations for vibrational spectra

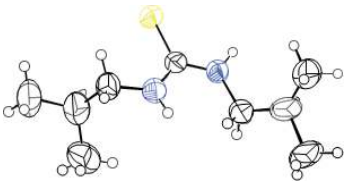

Figure 2. Crystal structure (ORTEP plot) of 1,3-diisobutyl thiourea compound.

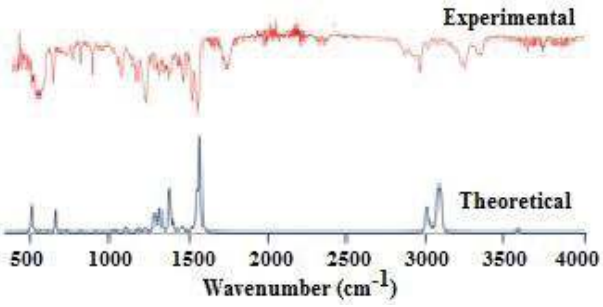

Figure 3. Comparative vibrational spectra of compound in gaseous state (theoretical, calculated using B3LYP/6–311G method) and in the solid state (experimental).

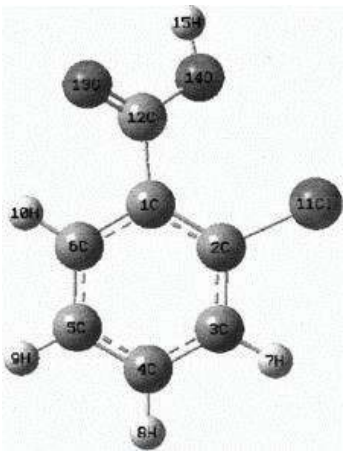

Figure 4. Numbering system implemented for 2-chlorobenzoic acid.

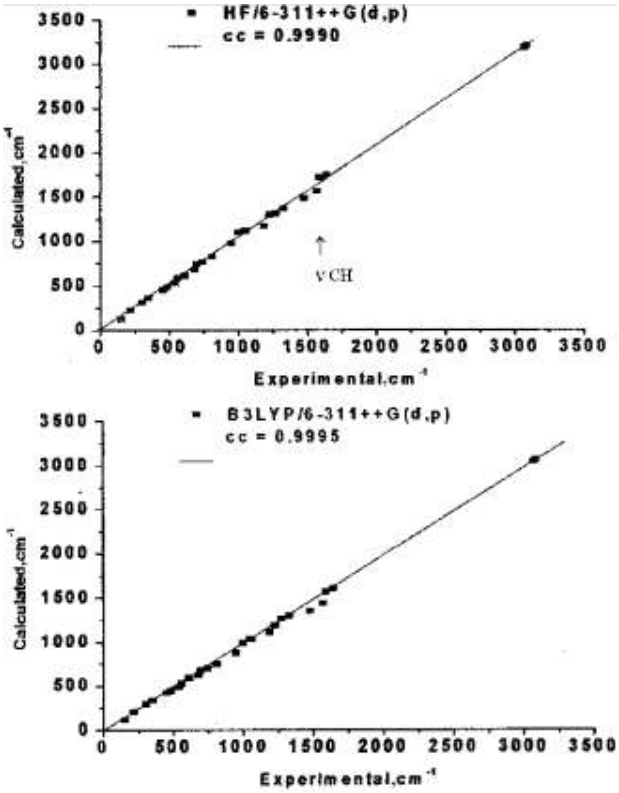

Figure 5. Graphic correlation between the experimental and calculated wavenumber obtained by the *ab initio* HF and DFT/B3LYP/6–311++G(d,p) methods for 2-chlorobenzoic acid.

analysis using DFT B3LYP/6–311G method were done in gaseous state, while experimental calculations were done in solid state. Geometry of compound was optimized using Gaussian employing DFT/B3LYP method with the 6–311G basis set. Optimized geometry of compound was compared with crystal structure of compound that depicted the support for the crystal structure (**Figure 2**). DFT results for vibrational analysis were compared with experimental analysis, which were found in good agreement with each other (**Figure 3**) [55].

Sundaraganesun et al., calculated structure, harmonic frequencies and vibrational mode assignments for 2-chlorobenzoic acid using HF and DFT methods employing the 6-311++G(d,p) basis set. The results of the molecular structure and vibrational frequencies obtained on the basis of calculations in Gaussian are critically equated with experimental IR data recorded in gas phase (**Figures 4** and **5**) [56].

6. Example illustrating calculation of NMR parameters

Alver et al. carried out NMR spectroscopic study, and DFT calculations of GIAO NMR shieldings and ^{1}J spin-spin coupling constants of 1,9-diaminononane (danon, $C_9H_{22}N_2$) were done. ^{1}H, ^{13}C NMR chemical shifts and $^{1}J_{CH}$ coupling constants of danon are calculated by means of B3LYP method, and 6-311++G(d,p) basis set is used. Comparison between the experimental and the theoretical results illustrates that density functional B3LYP method is able to deliver suitable results for expecting NMR properties (**Table 1**, **Figures 6** and **7**) [57].

Nuclei	Experimental (ppm)	B3LYP (ppm)
C_3, C_7	28.2	31.1
C_4, C_6	30.5	34.6
C_5	30.6	34.9
C_2, C_8	33.2	37.9
C_1, C_9	42.4	48.9
$H_{16,\ 17}$, $H_{24,\ 25}$	1.3	1.2
$H_{18,\ 19}$, $H_{22,\ 23}$, $H_{20,\ 21}$	1.3	1.3
$H_{30,\ 31}$, $H_{32,\ 33}$	1.5	1.2
$H_{14,\ 15}$, $H_{26,\ 27}$	1.5	1.3
$H_{12,\ 13}$, $H_{28,\ 29}$	2.6	2.5
$^{1}J(C_nH_n)$	**Experimental (Hz)**	**B3LYP (Hz)**
$C_2H_{14}H_{15}$, $C_8H_{26}H_{27}$	122.4	118.2
$C_3H_{16}H_{17}$, $C_7H_{24}H_{25}$	122.9	119.1
$C_4H_{18}H_{19}$, $C_6H_{22}H_{23}$	123.8	119.7
$C_5H_{20}H_{21}$, $C_1H_{12}H_{13}$, $C_9H_{28}H_{29}$	135.2	132.1

Table 1. Experimental and calculated ^{13}C, ^{1}H NMR chemical shifts (ppm) and $^{1}J_{CH}$ NMR coupling constants (Hz) of danon.

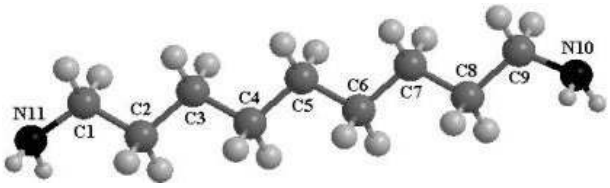

Figure 6. Optimized molecular structure of danon.

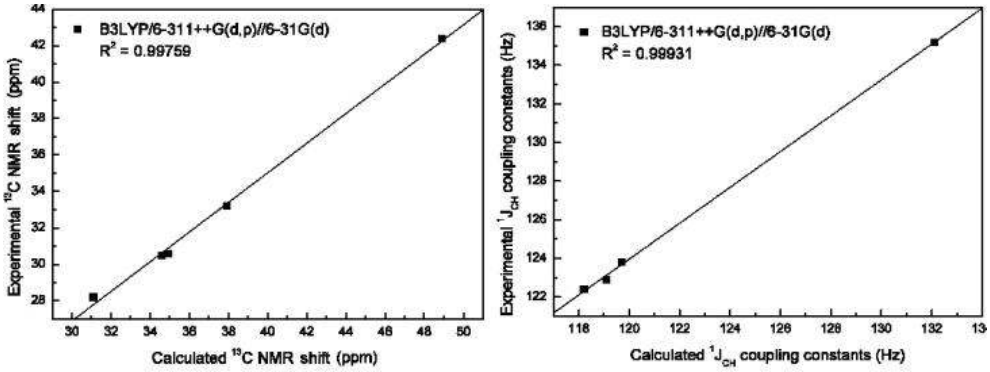

Figure 7. Plot of the calculated vs. the experimental ^{13}C NMR chemical shifts (ppm) and ^{1}J coupling constants (Hz) of danon.

6.1. Different software for DFT calculations

Gaussian is most extensively used software as graphical demonstration of variability of results, e.g., simulation of normal modes, molecular orbital, atomic charges, electrostatic potential, NMR shielding density and potential energy surface scans, can be displayed. Besides this, **Octopus** is a scientific program aimed at the ab initio virtual experimentation. Electrons are described quantum-mechanically within DFT and TDDFT when doing simulations in time. **Spartan** is a potent software tool that applies the power of molecular mechanics and quantum chemical calculations on chemistry research with sophisticated computational algorithms. **Dalton** is a powerful molecular electronic structure program, with an extensive functional for the calculation of molecular properties at the HF, DFT, MCSCF and CC levels of theory. **DMol3** is a unique, accurate and reliable DFT quantum mechanical code for research in the chemical and pharmaceutical industries. **CASTEP** is a software package that uses DFT to provide a good atomic level description of all manner of materials and molecules. It can give information about total energies, forces and stresses on an atomic system, as well as calculate optimum geometries, band structures, optical spectra, phonon spectra and much more. Dynamic simulations can be performed also. **HyperChem** software includes molecular mechanics, molecular dynamics, and semi-empirical and ab initio molecular orbital methods. HyperChemData and HyperNMR have been migrated into HyperChem and new features have been added.

7. Conclusion

This chapter focused on the use of DFT-based methods for spectral calculations, i.e., of vibrational, NMR and electronic calculations. Vibrational spectral generation depends upon Gaussian broadening function, while vibrational frequencies are calculated by determining the second derivative of energy after geometry optimization. Vibrational frequencies and zero-point energy for maximum vibration can be calculated theoretically as well. B3LYP density functional hybrid method is proposed to give more exact values of vibrational frequencies. The calculation of NMR parameters on DFT grounds depends upon exchange correlation functional, i.e., LDA, GGA and mostly employed hybrid functional B_3LYP. The GIAO and IGLO methods are used to solving gauge problems in NMR shielding tensor calculations. Nuclear spin-spin coupling constants can be calculated on theoretical grounds, whereas DFT-B3LYP-GIAO method is employed for chemical shift calculations. For electronic spectral calculations, TD-DFT is employed for excited state measurements. Vertical excitations, oscillator strength and intensity of absorption are calculated using TD-DFT theoretical methods. Linear response function incorporation to TD-DFT approach has proved helpful to study electronic density and absorption spectrum calculations of larger systems. Gaussian software is most employed for IR, NMR and UV spectral calculations.

Author details

Ataf Ali Altaf[1]*, Samia Kausar[1] and Amin Badshah[2]

*Address all correspondence to: atafali.altaf@uog.edu.pk

1 Department of Chemistry, University of Gujrat, Gujrat, Pakistan

2 Department of Chemistry, Quaid-i-Azam University, Islamabad, Pakistan

References

[1] Becke AD. A new mixing of Hartree-Fock and local density-functional theories. The Journal of Chemical Physics. 1993;**98**:1372-1377. DOI: 10.1063/1.464304

[2] Hohenberg P, Kohn W. Inhomogeneous electron gas. Physical Review. 1964;**136**:B864. DOI: 10.1103/PhysRev.136.B864

[3] Johnson BG. Development, implementation and applications of efficient methodologies for density functional calculations. Theoretical and Computational Chemistry. 1995;**2**: 169-219. DOI: 10.1016/S1380-7323(05)80036-6

[4] Kohn W, Sham LJ. Self-consistent equations including exchange and correlation effects. Physical Review. 1965;**140**:A1133. DOI: 10.1103/PhysRev.140.A1133

[5] Seminario JM. An introduction to density functional theory in chemistry. Theoretical and Computational Chemistry. 1995;**2**:1-27. DOI: 10.1016/S1380-7323(05)80031-7

[6] Watson TM, Hirst JD. Density functional theory vibrational frequencies of amides and amide dimers. The Journal of Physical Chemistry A. 2002;**106**:7858-7867. DOI: 10.1021/jp025551l

[7] Wong MW. Vibrational frequency prediction using density functional theory. Chemical Physics Letters. 1996;**256**:391-399. DOI: 10.1016/0009-2614(96)00483-6

[8] Malkin VG. Nuclear magnetic resonance shielding tensors calculated with a sum-over-states density functional perturbation theory. Journal of the American Chemical Society. 1994;**116**:5898-5908. DOI: 10.1021/ja00092a046

[9] Kutzelnigg W, Fleischer U, Schindler M. The IGLO-method: Ab-initio calculation and interpretation of NMR chemical shifts and magnetic susceptibilities. In: Deuterium and Shift Calculation. Verlag, Heidelberg: Springer; 1990. pp. 165-262

[10] Stratmann RE, Scuseria GE, Frisch MJ. An efficient implementation of time-dependent density-functional theory for the calculation of excitation energies of large molecules. The Journal of Chemical Physics. 1998;**109**:8218-8224. DOI: 10.1063/1.477483

[11] Alvarellos J, Metiu H. The evolution of the wave function in a curve crossing problem computed by a fast Fourier transform method. The Journal of Chemical Physics. 1988;**88**:4957-4966. DOI: 10.1063/1.454707

[12] Simoni E. Time-dependent theoretical treatment of intervalance absorption spectra. Exact calculations in a one-dimensional model. The Journal of Physical Chemistry. 1993;**97**: 12678-12684. DOI: 10.1021/j100151a009

[13] Franzen S. Use of periodic boundary conditions to calculate accurate β-sheet frequencies using density functional theory. The Journal of Physical Chemistry A. 2003;**107**:9898-9902. DOI: 10.1021/jp035215k

[14] Scott AP, Radom L. Harmonic vibrational frequencies: An evaluation of Hartree-Fock, Møller-Plesset, quadratic configuration interaction, density functional theory, and semi-empirical scale factors. The Journal of Physical Chemistry. 1996;**100**:16502-16513. DOI: 10.1021/jp960976r

[15] Levine IN, Busch DH, Shull H. Quantum Chemistry. 5th ed. Upper Saddle River NJ: Pearson Prentice Hall; 2009. p. 6

[16] Foresman JB. Ab initio techniques in chemistry: Interpretation and visualization. In: Swift ML, Zielinski TJ, editors. Ch. 14 in Using Computers in Chemistry and Chemical Education. Washington, DC: ACS Books; 1997

[17] Nagabalasubramanian P. FTIR and FT Raman spectra, vibrational assignments, ab initio, DFT and normal coordinate analysis of α,α dichlorotoluene. Spectrochimica Acta Part A: Molecular and Biomolecular Spectroscopy. 2009;**73**:277-280. DOI: 10.1016/j.saa.2009.02.044

[18] Becke AD. Density-functional exchange-energy approximation with correct asymptotic behavior. Physical Review A. 1988;**38**:3098. DOI: 10.1103/PhysRevA.38.3098

[19] Andersson MP, Uvdal P. New scale factors for harmonic vibrational frequencies using the B3LYP density functional method with the triple-ζ basis set 6-311+ G (d, p). The Journal of Physical Chemistry A. 2005;**109**:2937-2941. DOI: 10.1021/jp045733a

[20] Ernst RR, Bodenhausen G, Wokaun A. Principles of Nuclear Magnetic Resonance in one and two Dimensions. 2nd ed. Clarendon Press Oxford. 1987;**14**:640 p. ISBN: 0-19-855647-0

[21] Tossell JA. Nuclear Magnetic Shieldings and Molecular Structure. 2nd ed. Springer Netherlands: Springer Science & Business Media. 2012;**386**:584 p. DOI: 10.1007/978-94-011-1652-7

[22] Jensen F. Introduction to Computational Chemistry. United States: John Wiley & Sons; 2017

[23] Fukui H. Methods of calculating NMR chemical shifts. Magnetic Resonance Review. 1987;**11**:205-274

[24] Schreckenbach G, Ziegler T. The calculation of NMR shielding tensors based on density functional theory and the frozen-core approximation. International Journal of Quantum Chemistry. 1996;**60**:753-766. DOI: 10.1002/(SICI)1097-461X

[25] Parr RG, Weitao Y. Density-Functional Theory of Atoms and Molecules. Oxford University Press; 1994. p. 16

[26] McWeeny R. Methods of Molecular Quantum Mechanics. Academic Press; 1992

[27] Becke AD. Current-density dependent exchange-correlation functionals. Canadian Journal of Chemistry. 1996;**74**:995-997. DOI: 10.1139/V09-102

[28] Bru K, DFT Study of NMR Chemical Shifts and Spin-Spin Scalar Interactions in Nucleic Acids. National Centre for Biomolecular Research. 2003;9-81

[29] Perdew JP. Density-functional approximation for the correlation energy of the inhomogeneous electron gas. Physical Review B. 1986;**33**:8822. DOI: 10.1103/PhysRevB.33.8822

[30] Perdew JP, Pederson MR, Singh DJ, Fiolhais C, et al. Atoms, molecules, solids, and surfaces: Applications of the generalized gradient approximation for exchange and correlation. Physical Review B. 1992;**46**(6671):9

[31] Lee C, Yang W, Parr RG. Development of the Colle-Salvetti correlation-energy formula into a functional of the electron density. Physical Review B. 1988;**37**:785. DOI: 10.1103/PhysRevB.37.785

[32] Kutzelnigg W. Ab initio calculation of molecular properties. Journal of Molecular Structure: Theochem. 1989;**202**:11-61. DOI: 10.1016/0166-1280(89)87003-4

[33] Schreckenbach G, Ziegler T. Density functional calculations of NMR chemical shifts and ESR g-tensors. Theoretical Chemistry Accounts: Theory, Computation, and Modeling (Theoretica Chimica Acta). 1998;**99**:71-82. DOI: 10.1007/s002140050

[34] Schreckenbach G, Ziegler T. Calculation of NMR shielding tensors using gauge-including atomic orbitals and modern density functional theory. The Journal of Physical Chemistry. 1995;**99**:606-611. DOI: 10.1021/j100002a024

[35] Kutzelnigg W. Theory of magnetic susceptibilities and NMR chemical shifts in terms of localized quantities. Israel Journal of Chemistry. 1980;**19**:193-200. DOI: 10.1002/ijch.198000020

[36] Malkin VG. The calculation of NMR and ESR spectroscopy parameters using density functional theory. Theoretical and Computational Chemistry. 1995;**2**:273-347. DOI: 10.1016/S1380-7323(05)80039-1

[37] Malkin VG, Malkina OL, Salahub DR. Calculation of spin—Spin coupling constants using density functional theory. Chemical Physics Letters. 1994;**221**:91-99. DOI: 10.1016/0009-2614(94)87023-3

[38] Bagley AC. Investigations of NMR chemical shifts using DFT-B3LYP-GIAO calculations. In: NMR Spectroscopy in the Undergraduate Curriculum: Upper-Level Courses and across the Curriculum. Vol. 32016. ACS Publications. pp. 67-77. DOI: 10.1021/bk-2016-1225.ch005

[39] Runge E, Gross EK. Density-functional theory for time-dependent systems. Physical Review Letters. 1984;**52**:997. DOI: 10.1103/PhysRevLett.52.997

[40] Gross E, Kohn W. Time-dependent density-functional theory. Advances in Quantum Chemistry. 1990;**21**:255-291. DOI: 10.1016/S0065-3276(08)60600-0

[41] Gross E, Dobson J, Petersilka M. Density functional theory of time-dependent phenomena. Density Functional Theory II. 1996:81-172

[42] Casida ME, Huix-Rotllant M. Progress in time-dependent density-functional theory. Annual Review of Physical Chemistry. 2012;**63**:287-323. DOI: 10.1146/annurev-physchem-032511-143803

[43] Castro A. Octopus: A tool for the application of time-dependent density functional theory. 2006;**243**:2465-2488. DOI: 10.1002/pssb.200642067

[44] Jacquemin D. Absorption and emission spectra in gas-phase and solution using TD-DFT: Formaldehyde and benzene as case studies. Chemical Physics Letters. 2006;**421**:272-276. DOI: 10.1016/j.cplett.2006.01.068

[45] Rüger R. Efficient calculation of electronic absorption spectra by means of intensity-selected time-dependent density functional tight binding. Journal of Chemical Theory and Computation. 2014;**11**:157-167. DOI: 10.1021/ct500838h

[46] Makowska-Janusik M. Absorption spectra of poly-N-vinylcarbazole derivatives by experiment and simulation. European Polymer Journal. 2004;**40**:799-804. DOI: 10.1016/j.eurpolymj.2003.11.019

[47] Kityk I. Time-dependent DFT simulation of UV-spectra and molecular structure of several bis-pyrazolopyridines derivatives

[48] Adamo C, Jacquemin D. The calculations of excited-state properties with time-dependent density functional theory. Chemical Society Reviews. 2013;**42**:845-856. DOI: 10.1039/C2CS35394F

[49] Tussupbayev S. Comparison of real-time and linear-response time-dependent density functional theories for molecular chromophores ranging from sparse to high densities of states. Journal of Chemical Theory and Computation. 2015;**11**:1102-1109. DOI: 10.1021/ct500763y

[50] Brabec J et al. Fast algorithms for estimating the absorption spectrum within the linear response time-dependent density functional theory. 2015;1-19

[51] Rocca D. Turbo Charging time-dependent density-functional theory with Lanczos chains. The Journal of Chemical Physics. 2008;**128**:154105. DOI: 10.1063/1.2899649

[52] Chong DP. Recent Advances in Density Functional Methods: (Part I). Singapore: World Scientific; 1995. p. 1

[53] Petersilka M, Gossmann U, Gross E. Excitation energies from time-dependent density functional theory. Physical Review Letters. 1996;**76**:1212. DOI: 10.1103/PhysRevLett.76.1212

[54] Martin RL. Natural transition orbitals. The Journal of Chemical Physics. 2003;**118**:4775-4777. DOI: 10.1063/1.1558471

[55] Altaf AA. Synthesis, crystal structure, and DFT calculations of 1,3-diisobutyl thiourea. Journal of Chemistry. 2015;**2015**:1-5. DOI: 10.1155/2015/913435

[56] Sundaraganesan N, Joshua BD, Radjakoumar T. Molecular structure and vibrational spectra of 2-chlorobenzoic acid by density functional theory and ab-initio Hartree-Fock calculations. Indian Journal of Pure and Applied Physics. 2009;**47**:248-258

[57] Alver Ö, Parlak C, Senyel M. NMR spectroscopic study and DFT calculations of GIAO NMR shieldings and 1JCH spin-spin coupling constants of 1,9-diaminononane. Bulletin of the Chemical Society of Ethiopia. 2009;**23**:437-444. DOI: 10.4314/bcse.v23i3.47668